

Revision 2

Why Tolbachik diamonds cannot be natural

Konstantin D. Litasov^{1,2}, Hiroyuki Kagi³, Tatyana B. Bekker⁴,

Yoshiki Makino⁵, Takafumi Hirata³, Vadim V. Brazhkin¹

¹ *Institute for High Pressure Physics RAS, Troitsk, Moscow, Russia*

² *Fersman Mineralogical Museum RAS, Moscow, Russia*

³ *Geochemical Research Center, The University of Tokyo, Tokyo, Japan*

⁴ *Department of Geology and Geophysics, Novosibirsk State University, Novosibirsk, Russia*

⁵ *National Institute of Advanced Industrial Science and Technology, Tsukuba, Ibaraki, Japan*

ABSTRACT

Taking into account recent publications we provide additional comprehensive evidence that type Ib cuboctahedral diamonds and some other microcrystalline diamonds from Kamchatka volcanic rocks and alluvial placers cannot be natural and undoubtedly represent synthetic materials, which appear in the natural rocks by anthropogenic contamination. The major arguments provided in favor of the natural origin of those diamonds can be easily disproved. They include the coexistence of diamond and deltalumite from Koryaksky volcano; coexistence with super-reduced corundum and moissanite, Mn-Ni silicide inclusions, F-Cl enrichment and F/Cl-ratios, carbon and nitrogen isotopes in Tolbachik diamonds; microtwinning, Mn-Ni silicides and other inclusions in microcrystalline diamond aggregates for other Kamchatka placers. We emphasize the importance of careful comparison of unusual minerals found in nature, which include type Ib cuboctahedral diamonds and super-reduced phase assemblages resembling industrial slags, with synthetic analogs. The cavitation model proposed for the origin of Tolbachik diamonds is also unreliable since cavitation can cause the formation of nanosized diamonds only.

Keywords: diamond, Kamchatka, metal catalyst, silicide, super-reduced phases, cavitation, HPHT synthesis

INTRODUCTION

Recently, we presented comprehensive evidence that type Ib cuboctahedral diamonds from 2012-2013 eruption of Tolbachik volcano (Kamchatka) represent anthropogenic contamination based on the data on metallic inclusions, closely corresponding to the typical Mn₆₀Ni₄₀ catalyst used for the production of synthetic diamond in the Soviet Union / Russia (Litasov et al. 2019a;

35 Pokhilenko et al. 2019). We also argued that microcrystalline carbonado-like diamond aggregates
36 found in Kamchatka volcanoes and placers (Kaminsky et al. 2016; 2019) most likely represent
37 contamination by polycrystalline diamond compacts (PDC) and synthetic “carbonado” as they
38 contain Mn-Ni-Fe-bearing inclusions in the proportions of elements close to synthetic catalysts and
39 characteristic Si and SiC inclusions of bonding and reactionary materials used for the fabrication of
40 PDC (Litasov et al. 2020a). Finally, we emphasized the wide appearance of Ni₇₀Mn₂₅Co₅ metallic
41 inclusions in similar diamonds from ophiolite peridotite and chromitite, which also indicates their
42 appearance by anthropogenic contamination (Litasov et al. 2019a,b, 2020b) as this composition
43 (Ni₇₀Mn₂₅Co₅) corresponds to the widely used catalyst for synthetic diamond production in China.
44 Indeed, these papers caused extensive discussion and criticism (Yang et al. 2020; Kaminsky et al.
45 2020).

46 Galimov et al. (2020) provided new interesting data on type Ib cuboctahedral diamonds found
47 on the top of the lava flows at Tolbachik volcano and re-argued that they are of natural origin and
48 could be formed by chemical vapor deposition (CVD) or by hydrodynamic or acoustic cavitation in
49 the gas bubbles, which can collapse and generate intense shock waves. Consequently, we must once
50 again draw the attention of the scientific community to the problem of Tolbachik diamonds and
51 summarize below our criticism of the previously published conclusions (Karpov et al. 2014; Anikin
52 et al. 2018; Silaev et al. 2019a,b; Gordeev et al. 2019; Kaminsky et al. 2020) that these diamonds
53 are natural. In this manuscript, we provide additional comprehensive evidence that type Ib
54 cuboctahedral diamonds and some other microcrystalline diamonds from Kamchatka placers cannot
55 be natural and undoubtedly represent synthetic materials, which appear in the natural rocks by
56 anthropogenic contamination.

57

58 **SAMPLES AND ANALYTICAL METHODS**

59 This paper is devoted to the discussion and presentation of some additional original data on
60 synthetic diamonds and diamonds found at Tolbachik volcano. Thus, a detailed information on
61 analytical methods can be found in Litasov et al. (2019a) and only a brief summary is provided
62 here. The samples were characterized by Fourier Transform Infrared (FTIR) spectroscopy using a
63 Bruker VERTEX 70 spectrometer equipped with a HYPERION 2000 microscope at the Institute of
64 Geology and Mineralogy, Siberian Branch Russian Academy of Sciences (IGM SB RAS) in
65 Novosibirsk. Back-scattered electron images and chemical analysis of host rock minerals were
66 obtained using a MIRA 3 LMU scanning electron microscope (Tescan Orsay Holding) coupled with
67 an INCA energy-dispersive X-ray microanalysis system 450 equipped with the liquid nitrogen-free
68 Large area EDS X-Max-80 Silicon Drift Detector (Oxford Instruments Nanoanalysis Ltd) at IGM
69 SB RAS. The laser-ablation inductively-coupled plasma mass-spectrometry (LA-ICP-MS) data

70 were obtained using an in-house laser ablation system (Cyber Probe) combined with a Yb:KGW
71 femtosecond laser (CARBIDE, Light Conversion, Vilnius, Lithuania) and a galvanometric fast
72 scanning laser system at Geochemical Research Center, The University of Tokyo (Makino et al.,
73 2019). A focused ion beam (FIB) system (FEI Scios) was used to prepare thin cross-section foils of
74 approximately $15 \times 10 \times 0.1 \mu\text{m}$ for microtexture observation and elemental mapping of inclusions
75 using transmission electron microscopy (TEM) with a high-resolution energy-dispersive X-ray
76 (EDX) spectrometer. The TEM study was performed using JEOL JEM-2100F (Ehime University,
77 Matsuyama, Japan) operated at 200 kV and equipped with two CCD cameras (Gatan, Orius 200D
78 and UltraScan1000).

79

80 **RESULTS AND DISCUSSION**

81 **Diamond finding and coexistence with deltalumite**

82 Galimov et al. (2020) reported that about 500 diamond grains were recovered from the
83 powdery white coating of deltalumite on the basaltic lava sample from the Leningradskoe flow of
84 2012-2013 eruption of Tolbachik volcano. They show cubic or tetragonal carbon pieces on
85 deltalumite from Koryaksky volcano and claimed that this carbon is diamond without confirmation
86 (Fig.1a). Although diamond crystals can have cubic shapes, in association with deltalumite it is
87 more appropriate for unusual graphite (e.g., Korsakov et al. 2019) (Fig.1b). Deltalumite is also not
88 confirmed by the original data. The identification of diamond and deltalumite by EDX spectra alone
89 is not sufficient. Nevertheless, the authors conclude that an *in situ* coexistence of diamond with
90 deltalumite from Koryaksky volcano is the most important proof of the natural origin of diamonds
91 from Tolbachik and other Kamchatka volcanoes. It is difficult to understand how this unidentified
92 carbon grain from Koryaksky volcano can confirm the natural origin of cuboctahedral type Ib
93 diamonds from Tolbachik volcano.

94 We believe that deltalumite in diamond-bearing samples from Tolbachik and Koryaksky
95 volcano should first be confirmed by spectroscopic methods or by X-ray diffraction. The carbon
96 fragment in Fig.1a is very interesting and should also be identified at least by Raman spectroscopy.
97 It is clear that the morphology of this carbon fragment is completely different from Tolbachik
98 cuboctahedral diamonds. The confirmation of deltalumite in association with diamonds would be
99 extremely important because it clearly indicates that the assemblage cannot be related to high
100 pressures since deltalumite is a low-pressure phase (Wilson and McConnell 1980; Levin and
101 Brandon 1998).

102 Galimov et al. (2020) note that several tens of diamonds were collected from another place
103 near Naboko vent, a few were collected from the Toludskoe lava field and some from the lava of
104 the 1975 eruption, and that these diamonds have the same size and morphology as those from 2012-

105 2013 lava of Leningradskoe flow described in their paper. It seems that it is extremely important to
106 show data on these separately found diamonds for comparison of the infrared spectra and
107 composition of the microinclusions with those from Leningradskoe flow. Unfortunately, the authors
108 did not perform this important study.

109

110 ***P-T* stability field of Al₂O₃-deltalumite**

111 Deltalumite, δ -Al₂O₃, was discovered by Pekov et al. (2019) in rounded aggregates from
112 Tolbachik volcano. It is dimorphous to corundum α -Al₂O₃ and has a spinel superstructure with *P*-
113 *4m2* space group. The structural formula is (Al_{0.67}□_{0.33})Al₂O₄. It is a thermodynamically metastable
114 phase with a narrow *PT*-field of crystallization (Wilson and McConnell 1980; Levin and Brandon
115 1998). Different polymorphs of Al₂O₃ can be synthesized by heating of different aluminium
116 hydroxides. Each of them has own sequence of transformation in the temperature range of 250-1000
117 °C finalized by high-temperature corundum structure (Wefers and Misra, 1987).

118 The δ -Al₂O₃ is a member of boehmite sequence of transformations: boehmite, γ -AlOOH
119 (<500 °C) → γ -Al₂O₃ (500—700 °C) → δ -Al₂O₃ (700—900 °C) → θ -Al₂O₃ (900—1000 °C) → α -
120 Al₂O₃ (>1000 °C) (Wilson and McConnell 1980; Levin and Brandon 1998). In Tolbachik, the
121 formation of deltalumite may be connected to the reaction of fumarole gases with basaltic magma.
122 It is difficult to determine whether deltalumite was crystallized directly from the reaction or by
123 heating of boehmite and γ -Al₂O₃ (Pekov et al. 2019). The kinetics of transformation is sluggish. At
124 1000 °C, the δ -Al₂O₃ totally disappears in about 8 weeks (Wilson and McConnell 1980).

125 High-pressure transformation from boehmite to corundum was not studied; however, it may
126 be similar to that from diaspore to corundum. The kinetics of phase transitions is much faster with
127 increasing pressure, and boehmite becomes unstable relative to diaspore when pressure is applied
128 (e.g., Kennedy 1959). The transition from diaspore to corundum without intermediate phases occurs
129 at 0.18 GPa and 396 °C and at 1.5 GPa and 515 °C in less than 70 hours (e.g., Haas 1972;
130 Fockenberg et al. 1996), i.e., at much lower temperatures than the temperatures of deltalumite
131 existence at 1 atm. Thus, it is clear that diamond and deltalumite cannot be the syngenetic minerals
132 and “the most important proof of the natural origin of diamonds from Tolbachik” (Galimov et al.,
133 2020) is compromised.

134

135 **The phases coexisting with Tolbachik diamond**

136 In addition to the Al₂O₃-bearing phase, diamond coexists with a moissanite, corundum,
137 sulfides, Mn-Ni and Cu-Sn alloy, native iron, aluminum, silicon, and copper (Galimov et al. 2020).
138 Some other coexisting and associated minerals reported by Karpov et al. (2014) and Silaev et al.
139 (2019b) include Cu-Zn alloy, Fe-Ti-silicide, WC and many other phases. Some of the metallic

140 particles can be formed by volcanic activity and reactions with fumarole gases; however, they
141 should not be considered all together. For example, Cu, Cu-Sn, and Cu-Zn are common alloy
142 binders for diamond-WC and diamond-Fe abrasives and other industrial tools (e.g., Pekker et al.
143 1988; Gorbunov et al. 1990), whereas Fe-Ti-silicides is most common inclusions in Al₂O₃- and
144 SiC-based abrasives and ceramics (Litasov et al. 2019c).

145 However, the most convincing evidence for anthropogenic contamination, other than diamond
146 itself, is corundum with super-reduced (SR) inclusions. Silaev et al. (2019b) described Ti-bearing
147 corundum grains with TiN (hamrabaevite) and TiC (osbornite) and argue that they associate with
148 the diamond at Tolbachik volcano.

149 Recently, we discussed the possibility of anthropogenic contamination of alluvial deposits
150 near Mt Carmel (Israel) (Griffin et al. 2018a; 2019) by abrasive materials or industrial slags after
151 ferroalloy production (Litasov et al. 2019c,d). The grains of fused alumina and corundum from Mt
152 Carmel contained nearly the same mineral assemblage, which includes Ti₂O₃-tistarite, Ti₄Al₂ZrO₁₁-
153 carmeltazite, Fe-Si-Ti-alloys, TiN_{1-x}, and TiC_{1-x}. Similar Ti-bearing corundum grains with tistarite,
154 carmeltazite, Fe-Si-Ti-alloys, TiN, Ti-Si-nitrophosphides, were described in mineral concentrates
155 from Tibet ophiolite (Xu et al. 2013; 2015).

156 Tatarintsev et al. (1987) studied heavy mineral concentrate from Devonian volcanic breccia
157 and Quaternary alluvial deposits of the Donetsk region, which also contain also small remnants of
158 garnet peridotites and mantle minerals, such as pyrope, Cr-spinel, and picroilmenite. The SR phases
159 are represented by metallic iron, Mn-silicides, Fe- and Ti-carbides, moissanite and Ti-bearing
160 corundum. The microinclusions in corundum contain spinel, Fe-Ti-silicides, silicates, anorthite
161 glass, perovskite, TiN and carmeltazite (which they named Ti-Al-Zr phase).

162 How can Ti-bearing corundum with SR inclusions, which is equivalent to industrial fused
163 alumina (Litasov et al., 2019c) crystallize in such different geological environments? Griffin et al.
164 (2018b) argued that all these findings indicate the widespread occurrence and natural origin of
165 corundum with SR inclusions, however, a reliable model of the origin is difficult to constrain and
166 moreover it should be nearly similar for very contrast geological environments, whereas similarities
167 with industrial alumina-bearing slags are very clear (Litasov et al., 2019c,d). Ballhaus et al. (2017)
168 proposed a lightning strike hypothesis for the origin of the SR phases, but it is applicable to μm-
169 sized crystals and hardly explains the observed mineral assemblages with a relatively large grain
170 size up to several centimeters.

171

172 **Microinclusions in Tolbachik diamonds and “kamchatites”**

173 Galimov et al. (2020) determined similar compositions of metallic inclusions in Tolbachik
174 diamonds to those reported by Litasov et al. (2019), however, they provided more comprehensive

175 data. They show that: (a) Mn-Ni inclusions vary in composition from MnNi to Mn₂Ni with 45-67
176 wt.% Ni, (b) the Mn-Ni inclusions contain up to 5 wt.% Si, (c) Silicides with 19 at.% Si were
177 found in polycrystalline carbonado-like aggregates from other placers in Kamchatka (Kaminsky et
178 al. 2019), and (d) various Mn-silicides appear in the inclusions, which were not reported for
179 synthetic diamonds before based on very limited reference data (Bezrukov et al. 1972; Palyanov et
180 al. 1997; Lang 1995). Thus, Galimov et al. (2020) argued that the Si-bearing nature of metallic
181 inclusions in Tolbachik diamonds undoubtedly proves their natural origin.

182 In Litasov et al. (2019b), we show that trace element composition of the individual diamonds
183 can vary widely with respect to Mn/Ni ratio, from pure Mn to pure Ni. However, most analyses
184 show compositions that are close to those of catalyst. Similar data were obtained by X-ray
185 diffraction, where pure β - or γ -Mn, intermediate alloys and Ni₃Mn were recognized (e.g., Detchuev
186 et al. 1983). Yet, the average composition of Mn-Ni inclusions in diamonds from Tolbachik
187 reported by Galimov et al. (2020) is Mn₅₇Ni₄₃, which is very close to the Mn₆₀Ni₄₀ catalyst.

188 There are more than 50 papers devoted to microinclusions in synthetic diamonds published
189 only in Russian literature, which are available to the authors of Galimov et al. (2020). These papers
190 show that Si impurities are common for industrial synthetic diamonds. We can note only two
191 references, which show up to 0.2 wt.% Si in synthetic diamonds (with Mn = 0.3-0.4 wt.% and Ni =
192 0.4-0.6 wt.%) determined by emission spectroscopy (Otopkov et al. 1974) and similar data with
193 0.05-0.2 wt.% Si in diamonds (with Mn \approx 0.2 wt.% and Ni \approx 0.25 wt.%) determined by
194 instrumental neutron activation analysis (Novikov et al. 1987). These data indicate that Si/metal
195 ratios can be high enough to produce silicides in the inclusions. One additional study can be
196 mentioned where Vishnevsky et al. (1975) reported NiO, MnO, MnO₂, MnTiO₃, metallic γ -Ca, and
197 Ca-silicate or carbonate among inclusions in diamonds synthesized using Mn-Ni catalyst. The
198 inclusions were identified by X-ray diffraction.

199 Indeed, even in the papers cited by Galimov et al. (2020), we can find some additional
200 information. Bezrukov et al. (1972) noticed up to 5 wt% Fe and Si impurities in the Mn-Ni
201 inclusions from synthetic diamonds. Palyanov et al. (1996) described Fe-Ni metal, wüstite,
202 magnetite, chromite, and silicates (garnet, orthopyroxene) as inclusions in diamonds grown using
203 Fe-Ni catalyst. Lang et al. (1995) noticed Fe-Co inclusions coexisting with garnet and pyroxene
204 from synthetic diamond, which indicate the presence of Si in the growth medium. All authors
205 explained the appearance of silicates by the diffusion of surrounding materials into the melt and by
206 impurities in the initial chemical reagents. We also noticed a significant Si-content in synthetic
207 diamonds (Litasov et al., 2019b), however, quantitative calibration was difficult due to the high
208 SiO₂ content in the standard material. We can clearly see the signal from Si in the time-resolved
209 spectra during the LA-ICP-MS measurements both in Tolbachik and synthetic diamonds (Fig.2).

210 The intensity of the Si signal positively correlates with that from metal, and Si intensities in
211 Tolbachik diamonds are comparable with those from synthetic ones (Fig.3).

212 The possible source of Si-impurities in synthetic diamonds is very clear. It is either minor part
213 of Mn-Ni catalyst, which according to the GOST standard may contain up to 1.5 wt% Fe and Si
214 (Shipilo et al. 2005), or the high-pressure cell material used in diamond synthesis, “catlenite” or
215 “lithographic stone” (Zhigadlo, 2014), which is a well-sintered Ca-carbonate containing up to 15
216 wt% silicates. It was shown that this material can diffuse into the growth medium during industrial
217 synthesis (e.g., Davydov 1982, Litasov et al. 2019a). Importantly, Si, and even Ca, can be reduced
218 to metal during diamond synthesis and this is confirmed by original data (Vishnvesky et al. 1975).
219 It should be noted that pyrophyllite was also used as a pressure medium for similar experiments
220 (Zhang, 1986). In this case, the penetration of Si into the diamond growth medium is even more
221 obvious. We also analyzed several conventional Mn-Ni and Fe-Ni catalysts for synthetic diamond
222 growth and confirmed that the major impurities are represented by Si and Fe (for Mn-Ni) in the
223 amounts of up to 0.6 wt.% (Table 1).

224 Although Mn-silicides were not reported as inclusions in synthetic diamonds so far, it can be
225 emphasized that silicide phases were described in synthetic diamonds grown using the media other
226 than Mn-Ni alloy. Yin et al. (2000a,b), using transmission electron microscopy, observed
227 (Fe,Ni)₂₃C₆, FeSi₂, and SiC inclusions in diamonds grown from the Fe-Ni-C system. Later, similar
228 inclusions of Fe₃C, FeSi₂, SiO₂, and fcc-SiC were identified in diamonds grown in the Fe-C system
229 (Yin et al. 2001). All these data indicate that Mn/Ni-variability and Mn-silicides cannot be
230 considered as a specific natural feature of inclusions in Tolbachik diamonds.

231 The high-Si inclusions and interstitial Si and SiC described by Kaminsky et al. (2016; 2019)
232 in microcrystalline diamond aggregates from Kamchatka, named “kamchatite”, were discussed in
233 detail by Litasov et al. (2020a) and they have no similarities with the Tolbachik diamonds.
234 Kaminsky et al. (2020) ignore the facts that (a) diamond aggregates from Avacha volcano and
235 Aynyn river are completely different, the first represents synthetic “carbonado”, whereas the second
236 appears to be PDC prepared by impregnation of metallic Si into diamond powder (the images of
237 PDC can be found in Shulzhenko et al. 2000; Shimono and Kume 2004; Bolad and Li 2010); (b)
238 Mn-Ni silicides would be a common product of PDC fabrication, due to the migration of Mn-Ni
239 metallic inclusions in diamond crystals toward the surface during high-temperature annealing (e.g.,
240 Otopkov et al. 1974; Webb and Jackson 1995), and Mn/Ni ratio in these silicides perfectly matches
241 the Mn₆₀Ni₄₀ catalyst (Table 1); (c) almost all other inclusions and interstitial minerals, SiC, SiO₂,
242 Si, CaCO₃, β-Mn, W₂C, and B₄C match with industrially synthesized synthetic “carbonado” and
243 PDC; and (d) nano-twinning is a common phenomenon in synthetic diamonds (e.g., Malov 1971;
244 Westraadt et al. 2007). We emphasize that some minor features of microcrystalline diamond

245 aggregates are not yet explained by the synthetic origin, and the major mineral associated with the
246 purported diamonds, tilleyite (Kaminsky et al., 2019), has not been observed in synthetic diamonds.
247 Kaminsky et al. (2020) noticed that “drilling operations occur worldwide every day, but they never
248 produce tilleyite”. However, no one has investigated used industrial diamonds to find tilleyite.
249 Tilleyite is a very reasonable product of oxidation and contamination during the synthesis of PDC
250 or synthetic “carbonado” or may be formed during or after the use of a drill bit.

251 We should also emphasize that Fe-Ni inclusions observed in natural diamonds and mentioned
252 by Galimov et al. (2020) should not be directly extrapolated to Tolbachik diamonds, because they
253 have completely different characteristics. For example, E. Smith et al. (2016) described Fe-Ni-C-S
254 inclusions, which consist of Fe-Ni-metal, $(\text{Fe,Ni})_3\text{C}$ and FeS in type IIa diamonds. These metallic
255 aggregates coexist with majorite garnet and Ca-bearing minerals (walstromite, larnite, Ca-Ti
256 perovskite). In other reports (Haggerty 1975; Sobolev 1981) metallic Fe and Fe-Ni inclusions are
257 also associated with Fe-sulfide, which is a characteristic feature of the deep-seated diamonds.

258 Galimov et al. (2020) also provided the F/Cl ratio determined for one Tolbachik diamond
259 (0.39) and argue for a close relation of diamonds to the gases from the host lava, which have F/Cl =
260 0.37 (Zelensky et al. 2014). Statistics for such a conclusion based on data from a single diamond are
261 not enough. Surprisingly, the data reported by Galimov et al. (2020) in Table 1 indicate a ratio F/Cl
262 =0.19 in volcanic gases, whereas for Tolbachik lava Zelensky et al. (2014) reported an average F/Cl
263 ratio of 1.43.

264 These F/Cl ratios are not compared to F and Cl in synthetic diamonds. The pores around
265 metallic and silicide inclusions in transmission electron microscope (TEM) films are also enriched
266 by F, Cl, and O. This is a common feature for all thin diamond films. It is known that about 1/3 of
267 the surface bonds of the diamond can be saturated with H, F, or Cl. Oxygen is also important
268 surface impurity (Sappok and Boehm 1968). Fig.4 shows the TEM-EDX spectrum of the area
269 around small Mn-Ni inclusion in a synthetic diamond, which indicates a significant amount of F
270 and Cl.

271 Fig.5 shows the F- and Cl-enrichment of a Mn-Ni-Si inclusion in the Tolbachik diamond
272 described by Litasov et al. (2019a). The diamond surface itself is slightly enriched by F relative to
273 Cl in both synthetic and Tolbachik diamonds. This indicates that Secondary Ion Mass-Spectrometry
274 (SIMS) or LA-ICP-MS data can give any F/Cl ratio depending on the amount of the
275 microinclusions ablated under the laser beam. Thus, the F/Cl = 0.39 ratio for Tolbachik diamonds is
276 insufficient evidence for the comparison of the purported diamonds with the host lava or volcanic
277 gases from 2012-2013 eruption.

278 Similarly, a higher concentration of trace elements in ophiolitic diamonds relative to synthetic
279 one (Howell et al. 2015) is not a criterion for natural origin as stated by Galimov et al. (2020).

280 Litasov et al. (2019a) noticed that absolute values of the trace element concentrations in diamonds
281 with metallic inclusions have no meaning because they depend on the amount of inclusions
282 captured by the laser beam during analysis. The elemental ratios are instead important and in the
283 case of Tolbachik or ophiolitic diamonds they correlate with the compositions of catalyst used for
284 diamond synthesis (Litasov et al. 2020b).

285

286 **Infrared and cathodoluminescence spectroscopy**

287 The FTIR spectra of Tolbachik diamonds resemble those from synthetic diamonds and show
288 the abundance of single-nitrogen atom C-centers with total N-content of 100-500 ppm (Fig.6-7).
289 Diamonds from an ophiolite (Xu et al. 2017) rarely contain minor A-centers (Fig.6-7), which is also
290 possible for synthetic diamonds. Galimov et al. (2020) suggested that similar type Ib diamonds can
291 rarely be found in nature and noticed as an example those from the Kokchetav massif (Khachatryan
292 2013). We examined the single spectrum of a presumably Ib diamond from Kokchetav massif
293 reported by Khachatryan (2013) and found that it shows completely different peaks positions and
294 extremely low N-contents (Fig.6). In contrast, the Kokchetav diamonds reported in other works
295 always have significant amounts of A-centers corresponding to type Ib-IaA and in general contain
296 very high amounts of total nitrogen (Fig.7) (e.g., De Corte et al. 1998; Cartigny et al. 2004). The
297 lowest nitrogen aggregation reported for natural diamonds was observed in microdiamonds from
298 Dachine komatiites (French Guiana) (Cartigny 2010) and Zimmi alluvial deposits (West Africa)
299 (Smit et al. 2016; 2018). They may be comparable with Tolbachik and ophiolite diamonds by FTIR
300 spectra, but clearly have some other distinctive features, such as sulfide inclusions (Smit et al. 2016;
301 2018; C. Smith et al. 2016).

302 Some minor features from FTIR spectra of Tolbachik diamonds, such as bands near 1508 cm^{-1}
303 1 and broad band near 3400 cm^{-1} that are related to water impurities or surface contamination are
304 also common for the synthetic diamonds.

305 An explanation of the FTIR spectra for Tolbachik and especially for ophiolite diamonds is a
306 serious issue since they indicate very short residence time under high pressures and temperatures
307 (Evans and Qi 1982; Xu et al. 2017). Galimov et al. (2020) noticed that this can be explained by the
308 cavitation hypothesis, which is described below. Indeed, this idea does not stand up to criticism.
309 Fig.8 shows cathodoluminescence images of Tolbachik and synthetic diamonds with clear sectorial
310 growth zones, which without a doubt, is impossible for fast non-directional growth in a cavitation
311 bubble.

312

313 **Other evidence for the natural origin of Tolbachik diamonds**

314 Carbon isotope measurements for Tolbachik diamonds are not informative as all type Ib
315 diamonds (with FTIR spectra similar to standard synthetic diamonds) found in nature, including
316 those from ophiolites worldwide, have low $\delta^{13}\text{C}$ values in the range from -22 to -30‰ (Karpov et al.
317 2014; Xu et al. 2017) resembling the range for synthetic diamonds (Boyd et al. 1988; Reutsky et al.
318 2008; Xu et al. 2017). Rarely, this value in ophiolite diamonds is shifted to -17‰ (Xu et al. 2017).

319 Galimov et al. (2020) determined $\delta^{15}\text{N} = -2.3$ and -2.6 ‰ for two Tolbachik diamonds and
320 argue that these values are different from synthetic diamonds, which should all have atmospheric
321 $\delta^{15}\text{N} = 0$. This conclusion is not correct, because all previous measurements of $\delta^{15}\text{N}$ in synthetic
322 diamonds indicate wider range up to $\delta^{15}\text{N} = -2.5$ ‰ (Boyd et al. 1988), $\delta^{15}\text{N} = -5.6$ ‰ (Howell et al.
323 2015), and $\delta^{15}\text{N} = -10$ ‰ (Reutsky et al. 2008).

324 As we can see, the only reliable evidence of the natural origin of Tolbachik diamonds is the
325 assertion of their finding in nature with presumably impossible contamination by anthropogenic
326 materials. Even this single item of evidence becomes less sustainable taking into account the
327 findings of fused alumina with TiN and TiC inclusions (Litasov et al., 2019c), moissanite, and
328 industrial alloys (Cu, Cu-Sn, Al) (Pekker et al. 1988; Gorbunov et al. 1990) in the same probes
329 (Silaev et al. 2019a,b). All these materials may indicate anthropogenic contamination.

330

331 **A model for the origin**

332 A deep-seated origin of Tolbachik diamonds at static *PT*-conditions in the diamond stability
333 field is not applicable due to shallow location of magma chambers below Klyuchevskoy group
334 volcanoes and short residence time of diamond crystals in basaltic magma before complete
335 dissolution/oxidation (see Litasov et al. 2019a). The CVD model is also refuted by Galimov et al.
336 (2020) as not reliable for the origin of Tolbachik diamonds. Galimov et al. (2020) suggested a
337 cavitation model for the origin of Tolbachik diamonds by epitaxial crystallization from CH_4 -bearing
338 gas. No further explanations about the possibility of the cavitation synthesis of diamonds were
339 provided.

340 The cavitation hypothesis was proposed by Galimov (1973) to explain the origin of
341 kimberlitic diamonds during fast ascent in a magma channel when they encounter constrictions. The
342 limiting stage of crystal growth during the cavitation process is the duration of the shock wave
343 formed by the collapse of a cavitation bubble, which is in the range of microseconds. In other
344 words, it is not much different from the detonation synthesis of nanodiamonds (e.g., Baidakova,
345 2014). Thus, the cavitation model is not applicable for natural relatively large single-crystal
346 diamonds and it was carefully discussed by Frank et al. (1973) in their comment on Galimov
347 (1973). Similar arguments are still valid against the cavitation hypothesis during the formation of
348 Tolbachik diamonds.

349 Frank et al. (1973) noticed that Galimov (1973) ignored the fundamental difference in the rate
350 control between the martensitic transformation of crystals from one polymorphic modification to
351 another if the carbon source is graphite or other carbon phases. It is well known that the shock
352 transformation of graphite leads to the formation of thin lenses of nanocrystalline diamonds, such as
353 in the Popigai impact crater (e.g., Ohfuji et al. 2015). If the carbon source is different from graphite
354 one would need time for diffusive segregation of chemical constituents. Galimov (1973) estimates
355 the duration, t_c of dynamic pressure due to bubble collapse as 2×10^{-3} s (which is indeed
356 overestimated). In this time diffusive segregation could occur through a thickness of order x
357 $=(Dt_c)^{1/2}$, where D is the diffusion coefficient. With a fairly generous allowance of 10^{-8} m² s⁻¹ for D
358 we have $x = 4.5$ μm (Frank et al. 1973). One cannot expect sectorial growth of a 200-300 μm single
359 crystal with metallic inclusions in $10^{-6} - 10^{-3}$ s even during repeated cavitation episodes.

360 In the subsequent paper Galimov (1985) argued that kinetic limitations can be overcome by
361 recrystallization of diamonds by the post-deformation annealing (e.g., Laudise 1970; Humphreys et
362 al. 2017). The driving force of this process is accumulated elastic potential energy. The formation of
363 the single crystal occurs due to the migration of grain boundaries and enlargement of grain size.
364 This mechanism is useful for metals plastically deformed into a non-porous ingot, which further
365 recrystallizes during a long time by post-deformation annealing (e.g., Fe for 1-2 hours at 800 °C,
366 Glover and Sellars 1972). Nanocrystalline diamonds or other non-metal materials cannot be
367 deformed into homogenous ingot due to fracturing (Laudise 1970). Besides, post-deformation
368 annealing of diamonds is possible at temperatures of about 3000 °C for a long time, exceeding
369 hours. We conclude that the mechanism of post-deformation annealing does not work for single
370 crystal growth of diamonds at all. Thus, the major arguments against the cavitation hypothesis are
371 large grain size, sectorial growth of diamond crystals, and Mn-Ni-Si metallic inclusions, all features
372 of typical synthetic diamonds.

373 We should mention that cavitation synthesis of diamond is a very perspective direction, which
374 may be more favorable industrially than detonation synthesis. At present, there are at least three
375 reports of diamond crystallization during the cavitation process (Flynn 1986; Galimov et al. 2004;
376 Khachatryan et al. 2008). The crystals were usually nanocrystalline and were identified by X-ray
377 diffraction and Raman spectroscopy. However, Khachatryan et al (2008) reported the formation of
378 5-10 μm diamond particles after repeated loading of the growth chamber by cavitation fluid
379 (aromatic compounds). Yet, there was no detailed characterization of those diamonds with
380 transmission electron microscopy.

381

382 **IMPLICATIONS**

383 We argue that the cuboctahedral type Ib diamond found in Tolbachik volcano and described
384 in many recent papers including detailed studies by Litasov et al. (2019a) and Galimov et al. (2020)
385 have an anthropogenic origin. Taking into account the above discussion, the arguments in favor of
386 the formation of Tolbachik diamonds in nature become rather negligible. There are still many
387 unusual geological findings of diamonds in non-traditional environments and we believe that their
388 study should be performed by close collaboration of field geologists with specialists in material
389 science and synthetic diamonds, who can help to distinguish between natural and synthetic
390 materials and perform experiments, which can shed a light on the problem. At present, we believe
391 that the amount of similarities between diamonds from Kamchatka and synthetic type Ib diamond is
392 more than enough and leaves little space for further speculations about their origin.

393 We highlight the need to perform a more careful examination of diamonds and carbon phases
394 from different locations in Kamchatka along with detailed trace element and spectroscopic
395 characteristics of such important minerals as corundum and moissanite with the subsequent study of
396 their microinclusions. These observations and measurements then need to be critically compared
397 with industrially produced analogs. The finding of the unusual minerals in nature does not exclude
398 anthropogenic factors. We emphasize that none of the described minerals were found *in situ* in the
399 basaltic rocks of Kamchatka.

400 Another important problem in description of diamonds from Tolbachik (Litasov et al. 2019a;
401 Galimov et al. 2020), microcrystalline diamonds from other Kamchatka placers (Kaminsky et al.
402 2016; 2019; Litasov 2020a), diamonds from ophiolite peridotite and chromitite (Howell et al. 2015;
403 Xu et al. 2017; Lian and Yang 2019; Litasov et al. 2019b), some diamonds in metamorphic rocks
404 (Farre-de-Pablo et al 2019; Massone 2019), and SR mineral assemblages from alluvium (Griffin et
405 al. 2018a,b; 2019; Litasov et al. 2019c,d) is that authors of original reports tend to mix all evidence
406 from different rock types and environments together. We show that in many cases the phases from
407 heavy concentrates, diamonds, SR minerals, and metals, have no relations to each other (Litasov et
408 al. 2020a,b). Every case should be carefully considered. There were many examples when new
409 geological findings were approved or disproved with the appearance of additional evidence. We
410 believe that the next important step is the detailed study of moissanite, which was found in many
411 rocks around the globe (e.g., Lyakhovich 1980; Di Pierro et al. 2003; Zhang et al. 2016;
412 Dobrzhinetskaya et al. 2018), and it is very difficult to determine its natural or artificial origin.

413

414 **ACKNOWLEDGEMENTS**

415 We thank C. Ballhaus and V.S. Kamenetsky for valuable comments and P. Cartigny and K.
416 Smit for help with the interpretation of the FTIR spectra.

417

418 **FUNDING**

419 Our work on type Ib and other non-traditional diamonds is partially supported by the state
420 assignment of IHPP RAS.

421

422 **REFERENCES CITED**

423 Anikin, L.P., Silaev, V.I., Chubarov, V.M., Petrovsky, V.A., Vergasova, L.P., Karpov, G.A.,
424 Sokorenko, A.V., Ovsyannikov, A.A., and Maksimov, A.P. (2018) Diamond and other
425 accessory minerals in the products of eruption in 2008–2009. Koryaksky volcano
426 (Kamchatka), Vestnik of the Institute of Geology of the Komi Science Center UB RAS, 32,
427 18–27 (in Russian). <https://doi.org/10.19110/2221-1381-2018-2-18-27>

428 Baidakova, M.V., 2014. Methods of characterization and models of nanodiamond particles. In: Vul,
429 A. and Shenderova, O. (Eds.), Detonation nanodiamonds: Science and applications. CRC
430 Press, Boca Raton, FL, pp. 73-99.

431 Ballhaus, C., Wirth, R., Fonseca, R.O.C., Blanchard, H., Pröll, W., Bragagni, A., Nagel, T.,
432 Schreiber, A., Dittrich, S., and Thome, V. (2017) Ultra-high pressure and ultra-reduced
433 minerals in ophiolites may form by lightning strikes. *Geochemical Perspectives Letters*, 5, 42-
434 46.

435 Bezrukov, G.N., Butuzov, V.P., Khatelishvili, G.V., and Chernov, D.B. (1972) Study of the
436 composition of inclusions in synthetic diamond crystals by microanalysis. *Soviet Physics-*
437 *Doklady*, 17, 421-424 (*Doklady USSR Academy of Science*, 204(1), 84-87, in Russian).

438 Boland, J.N. and Li, X.S. (2010) Microstructural characterisation and wear behaviour of diamond
439 composite materials. *Materials*, 3(2), 1390-1419.

440 Boyd, S.R., Pillinger, C.T., Milledge, H.J., Mendelsohn, M.J., and Seal, M. (1988) Fractionation of
441 nitrogen isotopes in a synthetic diamond of mixed crystal habit. *Nature*, 331, 604-607.

442 Cartigny, P., Chinn, I., Viljoen, K.F., and Robinson, D. (2004) Early Proterozoic ultrahigh pressure
443 metamorphism: evidence from microdiamonds. *Science*, 304, 853-855.

444 Cartigny, P. (2010) Mantle-related carbonados? Geochemical insights from diamonds from the
445 Dachine komatiite (French Guiana). *Earth and Planetary Science Letters*, 296(3), 329-339.

446 Davydov, V.A., Revin, O.G., and Slesarev, V.N. (1982) Diffusion of lithographic stone into
447 graphite at high pressures and temperatures. *Journal of Superhard Materials*, 18(3), 3-7.

448 De Corte, K., Cartigny, P., Shatsky, V.S., Sobolev, N.V., and Javoy, M. (1998) Evidence of fluid
449 inclusions in metamorphic microdiamonds from the Kokchetav massif, northern Kazakhstan.
450 *Geochimica et Cosmochimica Acta*, 62, 3765-3773.

451 Detchuev, Y.A., Zadnevrovsky, B.I., Laptev, V.A., Melekh, M.V., Repnikova, E.A., Shivrín, O.N.,
452 and Samoylovich, M.I. (1983) Study of the phase composition of inclusions in single crystals

- 453 of synthetic diamonds doped by electrically active impurities. *Diamonds and Superhard*
454 *Materials*, 13(5), 1-2.
- 455 Di Pierro, S., Gnos, E., Grobety, B.H., Armbruster, T., Bernasconi, S.M., and Ulmer, P. (2003)
456 Rock-forming moissanite (natural α -silicon carbide). *American Mineralogist*, 88, 1817-1821.
- 457 Dobrzhinetskaya, L., Mukhin, P., Wang, Q., Wirth, R., O'Bannon, E., Zhao, W., Eppelbaum, L.,
458 and Sokhonchuk, T. (2018) Moissanite (SiC) with metal-silicide and silicon inclusions from
459 tuff of Israel: Raman spectroscopy and electron microscope studies. *Lithos*, 310, 355-368.
- 460 Evans, T. and Qi, Z. (1982) The kinetics of the aggregation of nitrogen atoms in diamond.
461 *Proceedings of the Royal Society of London A: Mathematical, Physical and Engineering*
462 *Sciences*, 381, 159-178.
- 463 Farré-de-Pablo, J., Proenza, J.A., González-Jiménez, J.M., Garcia-Casco, A., Colás, V., Roqué-
464 Rossell, J., Camprubí, A., and Sánchez-Navas, A. (2019) A shallow origin for diamonds in
465 ophiolitic chromitites. *Geology*, 47(1), 75-78.
- 466 Flynn, H.G., 1986. Method and means for converting graphite to diamond. US Patent 4,563,341.
- 467 Fockenberg, T., Wunder, B., Grevel, K.-D., and Burchard, M., 1996. The equilibrium diaspore-
468 corundum at high pressures. *European Journal of Mineralogy*, 8, 1293-1299.
- 469 Frank, F.C., Lang, A.R., and Moore, M., 1973. Cavitation as a mechanism for the synthesis of
470 natural diamonds. *Nature*, 246, 143-144.
- 471 Galimov, E.M. (1973) Possibility of natural diamond synthesis under conditions of cavitation,
472 occurring in a fast-moving magmatic melt. *Nature*, 243, 389-391.
- 473 Galimov, E.M. (1985) Some evidences of reality of the cavitation synthesis of diamonds in nature.
474 *Geochemistry International*, 33(5), 456-471.
- 475 Galimov, E.M., Kaminsky, F.V., Shilobreeva, S.N., Sevastyanov, V.S., Voropaev, S.A.,
476 Khachatryan, G.K., Wirth, R., Schreiber, A., Saraykin, V.V., Karpov, G.A., and Anikin, L.P.
477 (2020) Enigmatic diamonds from the Tolbachik volcano, Kamchatka. *American Mineralogist*,
478 105, 498-509.
- 479 Galimov, E.M., Kudin, A.M., Skorobogatskii, V.N., Plotnichenko, V.G., Bondarev, O.L., Zarubin,
480 B.G., Strazdovskii, V.V., Aronin, A.S., Fisenko, A.V., and Bykov, I.V. (2004) Experimental
481 corroboration of the synthesis of diamond in the cavitation process. *Doklady Physics*, 49(3),
482 150-153.
- 483 Glover, G. and Sellars, C.M. (1972) Static recrystallization after hot deformation of α iron.
484 *Metallurgical Transactions*, 3(8), 2271-2280.
- 485 Gorbunov, A.E., Tsermen, S.I., and Pekker, I.S. (1990) Copper-tin binders for diamond tools. In:
486 *Perspective directions for application of diamond tools in engineering*. Kolchemanov N.A.
487 Ed., VNIILMAZ, Moscow, 61-69 (In Russian).

- 488 Gordeev, E.I., Silaev, V.I., Karpov, G.A., Anikin, L.P., Vasiliev, E.A., Sukharev, A.E. (2019) On
489 the history of the discovery and nature of diamonds in volcanic rocks of Kamchatka. Bulletin
490 of Perm State University: Geology, 18(4), 307-331 (In Russian).
491 <https://doi.org/10.17072/psu.geol.18.4.307>.
- 492 Griffin, W.L., Gain, S.E.M., Bindi, L., Toledo, V., Cámara, F., Saunders, M., and O'Reilly, S.Y.
493 (2018a) Carmeltazite, $ZrAl_2Ti_4O_{11}$, a new mineral trapped in corundum from volcanic rocks
494 of Mt Carmel, Northern Israel. Minerals, 8(12), 601.
- 495 Griffin, W.L., Huang, J.-X., Thomassot, E., Gain, S.E.M., Toledo, V., and O'Reilly, S.Y. (2018b)
496 Super-reducing conditions in ancient and modern volcanic systems: sources and behaviour of
497 carbon-rich fluids in the lithospheric mantle. Mineralogy and Petrology, 112(1), 101-114.
- 498 Griffin, W.L., Gain, S.E., Huang, J.-X., Saunders, M., Shaw, J., Toledo, V., and O'Reilly, S.Y.
499 (2019) A terrestrial magmatic hibonite-grossite-vanadium assemblage: Desilication and
500 extreme reduction in a volcanic plumbing system, Mount Carmel, Israel. American
501 Mineralogist: Journal of Earth and Planetary Materials, 104(2), 207-219.
- 502 Haas, H. (1972) Diaspore-corundum equilibrium determined by epitaxis of diaspore on corundum.
503 American Mineralogist, 57, 1375-1385.
- 504 Haggerty, S.E. (1975) The chemistry and genesis of opaque minerals in kimberlites. Physics and
505 Chemistry of the Earth, p. 295-307.
- 506 Howell, D., Griffin, W.L., Yang, J., Gain, S., Stern, R.A., Huang, J.-X., Jacob, D.E., Xu, X., Stokes,
507 A.J., and O'Reilly, S.Y. (2015) Diamonds in ophiolites: Contamination or a new diamond
508 growth environment? Earth and Planetary Science Letters, 430, 284-295.
- 509 Humphreys, J., Rohrer, G.S., and Rollett, A. (2017) Recrystallization and related annealing
510 phenomena, 3rd ed. Elsevier, 704 pp.
- 511 Kaminsky, F.V., Wirth, R., Anikin, L.P., Morales, L., and Schreiber, A. (2016) Carbonado-like
512 diamond from the Avacha active volcano in Kamchatka, Russia. Lithos, 265, 222-236.
- 513 Kaminsky, F.V., Wirth, R., Anikin, L.P., and Schreiber, A. (2019) "Kamchatite" diamond aggregate
514 from northern Kamchatka, Russia: New find of diamond formed by gas phase condensation or
515 chemical vapor deposition. American Mineralogist, 104, 140-149.
- 516 Kaminsky, F.V., Wirth, R., Anikin, L.P., and Schreiber, A. (2020) On "Kamchatite" diamond
517 aggregate from northern Kamchatka, Russia: New find of CVD-formed diamond in nature -
518 Reply to K.D. Litasov, T.B. Bekker, and H. Kagi. American Mineralogist, 105(1), 144-145.
- 519 Karpov, G.A., Silaev, V.I., Anikin, L.P., Rakin, V.I., Vasil'ev, E.A., Filatov, S.K., Petrovskii, V.A.,
520 and Flerov, G.B. (2014) Diamonds and accessory minerals in products of the 2012–2013
521 Tolbachik Fissure Eruption. Journal of Volcanology and Seismology, 8(6), 323-339.

- 522 Kennedy, G.C. (1959) Phase relations in the system of $\text{Al}_2\text{O}_3\text{-H}_2\text{O}$ at high temperatures and
523 pressures. *American Journal of Science*, 257(8), 563-573.
- 524 Khachatryan, G.K. (2013) Nitrogen and hydrogen in diamond crystals in aspect of geological and
525 genetic and exploration problems of diamond deposits. *Otechestvennaya Geologia* (No 2), 29-
526 42 (In Russian).
- 527 Khachatryan, A.K., Aloyan, S.G., May, P.W., Sargsyan, R., Khachatryan, V.A., and Baghdasaryan,
528 V.S. (2008) Graphite-to-diamond transformation induced by ultrasound cavitation. *Diamond
529 and Related Materials*, 17(6), 931-936.
- 530 Korsakov, A.V., Rezvukhina, O.V., Jaszczak, J.A., Rezvukhin, D.I., and Mikhailenko, D.S. (2019)
531 Natural graphite cuboids. *Minerals*, 9(2), 110.
- 532 Lang, A.R. and Meaden, G.M. (1991) Complementary orientation-dependent distributions of 1.40
533 and 2.56 eV cathodoluminescence on vicinals on {111} in synthetic diamonds. *Journal of
534 Crystal Growth*, 108(1-2), 53-62.
- 535 Lang, A.R., Vincent, R., Burton, N.C., and Makepeace, A.P.W. (1995) Studies of small inclusions
536 in synthetic diamonds by optical microscopy, microradiography and transmission electron
537 microscopy. *Journal of Applied Crystallography*, 28(6), 690-699.
- 538 Laudise, R.A. (1970) *The growth of single crystals*. Prentice Hall, Inc., Englewood Cliffs, New
539 Jersey 367 pp.
- 540 Levin, I., and Brandon, D. (1998) Metastable alumina polymorphs: crystal structures and transition
541 sequences. *Journal of the American Ceramic Society*, 81, 1995-2012.
- 542 Lian, D. and Yang, J. (2019) Ophiolite-hosted diamond: A new window for probing carbon cycling
543 in the deep mantle. *Engineering*, 5(3), 406-420.
- 544 Litasov, K.D., Kagi, H., Voropaev, S.A., Hirata, T., Ohfuji, H., Ishibashi, H., Makino, Y., Bekker,
545 T.B., Sevastyanov, V.S., Afanasiev, V.P., and Pokhilenko, N.P. (2019a) Comparison of
546 enigmatic diamonds from the Tolbachik arc volcano (Kamchatka) and Tibetan ophiolites:
547 Assessing the role of contamination by synthetic materials. *Gondwana Research*, 75, 16-27.
- 548 Litasov, K.D., Kagi, H., Bekker, T.B., Hirata, T., and Makino, Y. (2019b) Cuboctahedral type Ib
549 diamonds in ophiolitic chromitites and peridotites: the evidence for anthropogenic
550 contamination. *High Pressure Research*, 39(3), 480-488.
- 551 Litasov, K.D., Kagi, H., and Bekker, T.B. (2019c) Enigmatic super-reduced phases in corundum
552 from natural rocks: Possible contamination from artificial abrasive materials or metallurgical
553 slags. *Lithos*, 340-341, 181-190.
- 554 Litasov, K.D., Bekker, T.B., and Kagi, H. (2019d) Reply to the discussion of “Enigmatic super-
555 reduced phases in corundum from natural rocks: Possible contamination from artificial

- 556 abrasive materials or metallurgical slags” by Litasov et al. (*Lithos*, v.340-341, p.181-190) by
557 W.L. Griffin, V. Toledo and S.Y. O’Reilly. *Lithos*, 348-349: 105170.
- 558 Litasov, K.D., Bekker, T.B., and Kagi, H. (2020a) “Kamchatite” diamond aggregate from northern
559 Kamchatka, Russia: New find of diamond formed by gas phase condensation or chemical
560 vapor deposition – Discussion. *American Mineralogist*, 105(1), 141-143.
- 561 Litasov, K.D., Bekker, T.B., Kagi, H., and Ohfuji, H. (2020b). Reply to the comment on
562 “Comparison of enigmatic diamonds from the Tolbachik arc volcano (Kamchatka) and
563 Tibetan ophiolites: Assessing the role of contamination by synthetic materials” by Litasov et
564 al. (2019) (*Gondwana Research*, 75, 16–27) by Yang et al. *Gondwana Research*, 79, 304-307.
- 565 Lyakhovich, V.V. (1980) Origin of accessory moissanite. *International Geology Review*, 22(8),
566 961-970.
- 567 Makino, Y., Kuroki, Y., and Hirata, T. (2019) Determination of major to trace elements in metallic
568 materials based on solid mixing calibration method using multiple spot-laser ablation-ICP-
569 MS. *Journal of Analytical Atomic Spectrometry*, 34, 1794-1799.
- 570 Malov, Y.V., (1971) Microstructure of artificial polycrystalline diamonds. *Soviet Physics*
571 *Crystallography*, 15(6), 1042-1044.
- 572 Massonne, H.J. (2019) A shallow origin for diamonds in ophiolitic chromitites: Comment. *Geology*,
573 47(8), e476.
- 574 Novikov, N.V., Kocherzhinsky, Y.A., Shulman, L.A., Ositinskaya, T.D., Malogolovets, V.G.,
575 Lysenko, A.V., Malnev, V.I., Nevstruev, G.F., Pugach, E.A., Bogatyreva, G.P., and
576 Vishnevsky, A.S. (1987) Physical properties of diamonds, Handbook. Kiev, Naukova Dumka,
577 188 p. (in Russian).
- 578 Ohfuji, H., Irifune, T., Litasov, K.D., Yamashita, T., Isobe, F., Afanasiev, V.P., and Pokhilenko,
579 N.P. (2015) Natural occurrence of pure nano-polycrystalline diamond from impact crater.
580 *Scientific Reports*, 5, 14702.
- 581 Otopkov, P.P., Nozhkina, A.V., Vasil’eva, L.A., Dul’kina, L.A., Kostikov, V.I., and Andropov,
582 Y.I., (1974) The effect of heat treatment on physical and chemical properties of diamonds. In
583 *Physical and chemical properties of diamonds, Proceedings of VNIIALMAZ, Moscow*, 3, 15-
584 32 (In Russian).
- 585 Pal’yanov, Y.N., Khokhryakov, A.F., Borzdov, Y.M., Sokol, A.G., Gusev, V.A., Rylov, G.M., and
586 Sobolev, N.V. (1997) Growth conditions and real structure of synthetic diamond crystals.
587 *Russian Geology and Geophysics*, 38(5), 882-906.
- 588 Pal’yanov, Y.N., Khokhryakov, A.F., Borzdov, Y.M., Doroshev, A.M., Tomilenko, A.A., and
589 Sobolev, N.V. (1996) Inclusions in synthetic diamonds. *Transactions (Doklady) Academy of*
590 *Sciences: Earth Science Sections*, 341(3), 69-72.

- 591 Pekker, I.S., Gorbunov, A.E., Balkevich, V.L., Tserman, S.I., and Skidanenko A.I., (1988)
592 Activated sintering of composites of the diamond-copper-tin system. Soviet Powder
593 Metallurgy and Metal Ceramics, 27(12), 934-936.
- 594 Pekov, I. V., Anikin, L. P., Chukanov, N.V., Belakovskiy, D.I., Yapaskurt, V.O., Sidorov, E. G.,
595 Britvin, S. N., and Zubkova, N.V. (2019) Deltalumite, a new natural modification of alumina
596 with spinel-type structure. Zapiski RMO (Proceedings of the Russian Mineralogical Society)
597 148(5), 45-58 (In Russian).
- 598 Pokhilenko, N.P., Shumilova, T.G., Afanasiev, V.P., and Litasov, K.D. 2019. Diamond in the
599 Kamchatka peninsula (Tolbachik and Avacha volcanoes): Natural origin or contamination?
600 Russian Geology and Geophysics, 60 (5): 463-472.
- 601 Reutsky, V.N., Harte, B., Borzdov, Y.M., and Palyanov, Y.N. (2008) Monitoring diamond crystal
602 growth, a combined experimental and SIMS study. European Journal of Mineralogy, 20(3),
603 365-374.
- 604 Sappok, R., and Boehm, H.P. (1968) Chemie der oberfläche des diamanten—I benetzungswärmen,
605 elektronenspinresonanz und infrarotspektren der oberflächenhydride,-halogenide und-oxide.
606 Carbon, 6(3), 283-295.
- 607 Shimono, M. and Kume, S. (2004) HIP-Sintered Composites of C (Diamond)/SiC. Journal of the
608 American Ceramic Society, 87(4), 752-755.
- 609 Shipilo, V.B., Dutov, A.G., Komar, V.A., Shipilo, N.V., and Azarko, I.I. (2005) Crystallization of
610 diamonds in system Mn–Ni–C. Inorganic Materials, 41(3), 293-296.
- 611 Shulzhenko, A.A., Gargin, V.G., Bochechka, A.A., Oleinik, G.S., and Danilenko, N.V., (2000)
612 Diamond nanopowders used to improve strength of diamond- and silicon carbide-based
613 composites. Journal of Superhard Materials, 22(3), 3-15.
- 614 Silaev, V.I., Karpov, G.A., Anikin, L.P., Vasiliev, E.A., Vergasova, L.P., and Smoleva, I.V.
615 (2019a) Mineral phase paragenesis in explosive ejecta discharged by recent eruptions in
616 Kamchatka and the Kuril Islands. Part 1. Diamonds, carbonaceous phases, and condensed
617 organoids. Journal of Volcanology and Seismology, 13(5), 323-334.
- 618 Silaev, V.I., Karpov, G.A., Anikin, L.P., Vergasova, L.P., Filippov, V.N., and Tarasov, K.V.
619 (2019b) Mineral phase paragenesis in explosive ejecta discharged by recent eruptions in
620 Kamchatka and the Kuril Islands. Part 2. Accessory minerals of Tolbachik-type diamonds.
621 Journal of Volcanology and Seismology, 13(6), 323-334.
- 622 Smit, K.V., Shirey, S.B., and Wang, W. (2016) Type Ib diamond formation and preservation in the
623 West African lithospheric mantle: Re–Os age constraints from sulphide inclusions in Zimmi
624 diamonds. Precambrian Research, 286, 152-166.

- 625 Smit, K.V., D'Haenens-Johansson, U.F., Howell, D., Loudin, L.C., and Wang, W. (2018)
626 Deformation-related spectroscopic features in natural Type Ib-IaA diamonds from Zimmi
627 (West African craton). *Mineralogy and Petrology*, 112(1), 243-257.
- 628 Smith, E.M., Shirey, S.B., Nestola, F., Bullock, E.S., Wang, J., Richardson, S.H., and Wang, W.
629 (2016) Large gem diamonds from metallic liquid in Earth's deep mantle. *Science*, 354(6318),
630 1403-1405.
- 631 Smith, C.B., Walter, M.J., Bulanova, G.P., Mikhail, S., Burnham, A.D., Gobbo, L., and Kohn, S.C.
632 (2016) Diamonds from Dachine, French Guiana: A unique record of early Proterozoic
633 subduction. *Lithos*, 265, 82-95.
- 634 Sobolev, N.V., Efimova, E.S., and Pospelova, L.N. (1981) Native iron in diamonds of Yakutia and
635 its paragenesis. *Soviet Geology and Geophysics*, 22(12), 25-29.
- 636 Tatarintsev, V.I., Sandomirskaja, S., and Tsymbal, S.N. (1987). 1st find of titanium nitride
637 (osbornite) in rocks of the earth. *Transactions (Doklady) of the USSR Academy of Sciences:*
638 *Earth Science sections*, 296 (5-6), 155-159 (p.1458-1461, in Russian).
- 639 Vishnevsky, A.S., Lysenko, A.V., and Katsai, M.Y., (1975) Electronographic study of
640 microinclusions and phases in synthetic diamonds and reaction mixtures. *Synthetic*
641 *Diamonds*, 7(2), 7-13 (In Russian).
- 642 Webb, S.W., and Jackson, W.E. (1995) Synthetic diamond crystal strength enhancement through
643 annealing at 50 kbar and 1500 °C. *Journal of Materials Research*, 10(7), 1700-1709.
- 644 Westraadt, J.E., Dubrovinskaia, N., Neethling, J.H., and Sigalas, I. (2007) Thermally stable
645 polycrystalline diamond sintered with calcium carbonate. *Diamond and Related Materials*,
646 16(11), 1929-1935.
- 647 Wefers, K., and Misra, C. (1987) *Oxides and Hydroxides of Aluminum*. Alcoa Technical Paper No.
648 19. Alcoa Laboratories, Pittsburgh, PA, 92 pp.
- 649 Wilson, S. J., McConnell, J.D.C. (1980) A kinetic study of the system γ -AlOOH/Al₂O₃. *Journal of*
650 *Solid State Chemistry*, 34, 315-322.
- 651 Xu, X., Yang, J., Guo, G., and Xiong, F. (2013) Mineral inclusions in corundum from chromitites in
652 the Kangjinla chromite deposit, Tibet. *Acta Petrologica Sinica*, 29(6), 1867-1877.
- 653 Xu, X., Yang, J., Robinson, P.T., Xiong, F., Ba, D., and Guo, G. (2015) Origin of ultrahigh pressure
654 and highly reduced minerals in podiform chromitites and associated mantle peridotites of the
655 Luobusa ophiolite, Tibet. *Gondwana Research*, 27(2), 686-700.
- 656 Xu, X., Cartigny, P., Yang, J., Dilek, Y., Xiong, F., and Guo, G. (2017) Fourier transform infrared
657 spectroscopy data and carbon isotope characteristics of the ophiolite-hosted diamonds from
658 the Luobusa ophiolite, Tibet, and Ray-Iz ophiolite, Polar Urals. *Lithosphere*, 10(1), 156-169.

- 659 Yang, J., Simakov, S.K., Moe, K., Scribano, V., Lian, D., and Wu, W. (2020) Comment on
660 “Comparison of enigmatic diamonds from the tolbachik arc volcano (Kamchatka) and Tibetan
661 ophiolites: Assessing the role of contamination by synthetic materials” by Litasov et al.
662 (2019). *Gondwana Research*, 79, 301-303.
- 663 Yin, L.W., Zou, Z.D., Li, M.S., Liu, Y.X., Cui, J.J., and Hao, Z.Y. (2000) Characteristics of some
664 inclusions contained in synthetic diamond single crystals. *Materials Science and Engineering*
665 *A*, 293(1-2), 107-111.
- 666 Yin, L.W., Zou, Z.D., Li, M.S., Sun, D.S., Liu, Y.X., and Hao, Z.Y. (2000) Impurities identification
667 in a synthetic diamond by transmission electron microscopy. *Diamond and Related Materials*,
668 9(12), 2006-2009.
- 669 Yin, L.W., Li, M.S., Hao, Z.Y., and Zhang, J.F. (2001) Inclusions related to catalyst and medium
670 for transmitting pressure in diamond single crystals grown at high temperature and high
671 pressure from the Fe-C system. *Journal of Physics D*, 34(12), L57-L60.
- 672 Zelenski, M., Malik, N., and Taran, Y. (2014) Emissions of trace elements during the 2012–2013
673 effusive eruption of Tolbachik volcano, Kamchatka: enrichment factors, partition coefficients
674 and aerosol contribution. *Journal of Volcanology and Geothermal Research*, 285, 136-149.
- 675 Zhang, R.Y., Yang, J.-S., Ernst, W., Jahn, B.-M., Iizuka, Y., and Guo, G.-L. (2016) Discovery of in
676 situ super-reducing, ultrahigh-pressure phases in the Luobusa ophiolitic chromitites, Tibet:
677 New insights into the deep upper mantle and mantle transition zone. *American Mineralogist*,
678 101, 1245-1251.
- 679 Zhang, S. (1986) Some phenomena and analyses in growing diamond. *Journal of Crystal Growth*,
680 79, 542-546.
- 681 Zhigadlo, N. (2014) Spontaneous growth of diamond from MnNi solvent-catalyst using opposed
682 anvil-type high-pressure apparatus. *Journal of Crystal Growth*, 395, 1-4.
- 683
684
685

686

Figure captions

687

688 Fig.1. Cubic carbon fragment on deltalumite (?) from Koryaksky volcano (modified from Anikin et
689 al. 2018) (a) and cliftonite-like cubic graphite coexisting with kamacite from Ozernaya mountain
690 Fe-Ni-bearing basaltic intrusion (Norilsk, Russia) (modified from Korsakov et al. 2019).

691

692 Fig.2. Intensity of ^{13}C , ^{29}Si , ^{55}Mn , ^{57}Fe , and ^{60}Ni signals during LA-ICP-MS measurements of (a)
693 Tolbachik diamond (Litasov et al. 2019a) and (b) synthetic type Ib diamonds grown using
694 $\text{Ni}_{70}\text{Mn}_{25}\text{Co}_5$ catalysts (Litasov et al. 2019b).

695

696 Fig.3. Si versus metal (Fe+Mn+Ni) intensities of LA-ICP-MS measurements in Tolbachik and
697 synthetic type Ib diamonds grown using $\text{Ni}_{70}\text{Mn}_{25}\text{Co}_5$ (Litasov et al. 2019b) and other catalysts.

698

699 Fig.4. Example of TEM-EDX spectrum of the area around Mn-Ni inclusion in a synthetic diamond,
700 grown from Mn-Ni-C system and showing significant O, F, and Cl peaks. Insert show SEM image
701 of the inclusions and encircled analyzed spot. Cu and Ga are from TEM grid and ion beam,
702 respectively.

703

704 Fig.5. TEM-EDX element maps for Si, Cl, and F in the Mn-Ni inclusion in Tolbachik diamond (see
705 Fig.5 in Litasov et al. 2019a). Scale bar 100 nm.

706

707 Fig.6. FTIR spectra of type Ib and Ib-IaA diamonds from different sources: Synthetic diamonds
708 from (a) experiment with Mn-Ni catalyst at 6 GPa and 1400°C (b) saw grit and (c) used drill bit.
709 Tolbachik diamonds (Litasov et al. 2019a; Pokhilenko et al. 2019); diamonds from Tibet ophiolite
710 (Xu et al. 2018); diamonds from Zimmi alluvial deposits (West Africa) (Smit et al. 2016; 2018);
711 anomalous metamorphic diamond from Kokchetav massif (Khachatryan 2013). Note that most
712 typical metamorphic diamonds correspond to clear Ib-IaA type with significant degree of A-centers
713 aggregation.

714

715 Fig. 7. Nitrogen aggregation versus nitrogen content in Tolbachik (this work) and ophiolite-hosted
716 microdiamonds (Xu et al. 2017) in comparison with eclogite diamonds from kimberlite,
717 metamorphic diamonds (mainly from Kokchetav massif), microdiamonds from Akluilak minettes
718 (Canada) (Cartigny et al. 2004), diamonds from Dachine komatiite (French Guiana) and carbonado
719 (Cartigny 2010), and Zimmi (West Africa) alluvial diamond (Smit et al. 2016). Black line from 100
720 to 500 ppm N indicate a range observed in ophiolite diamonds, which coincide in general with that

721 for Tolbachik diamonds. Isoleths were calculated with the use of a residence time of 1 Ma for
722 temperatures ranging, by steps of 20°C, from 540° to 680°C (Evans and Qi 1982).

723

724 Fig.8. Cathodoluminescence images of Tolbachik diamond (modified from Karpov et al. 2014) and
725 synthetic diamonds grown on seed (modified from Lang and Meaden 1991) indicating sectorial
726 growth pattern typical for synthetic diamonds.

727

728

729

730 Table 1. Composition (wt.%) of industrial Mn-Ni and Fe-Ni catalysts for synthetic diamonds in
 731 USSR/Russia determined by energy-dispersive X-ray microanalysis.

	IHPP-1	IHPP-2	PRGN-40*	Ukraine	Belarus
N	16	14	20	10	10
Si	0.49 (6)	0.18 (3)	0.57 (8)	0.55 (9)	0.13 (4)
Ti	-	-	0.19 (4)	0.18 (6)	0.05 (3)
Cr	-	-	0.24 (5)	0.37 (4)	0.05 (4)
Mn	49.3 (0.8)	-	59.4 (1.0)	49.4 (7)	0.16 (5)
Fe	0.13 (4)	69.5 (1.1)	0.51 (8)	0.55 (12)	59.6 (1.0)
Co	0.17 (3)	0.14 (4)	-	0.21 (7)	-
Ni	49.5 (1.1)	29.8 (5)	38.9 (0.8)	49.1 (8)	40.2 (1.3)
Total	99.6 (1.0)	99.6 (8)	99.8 (1.0)	100.4 (9)	100.2 (1.1)

732 N – number of analyses. IHPP – Institute for High Pressure Physics. *Polema company. The alloys
 733 contain also minor carbon and oxygen. The standard deviation is in parentheses.

734

a



Carbon

Deltalumite ?

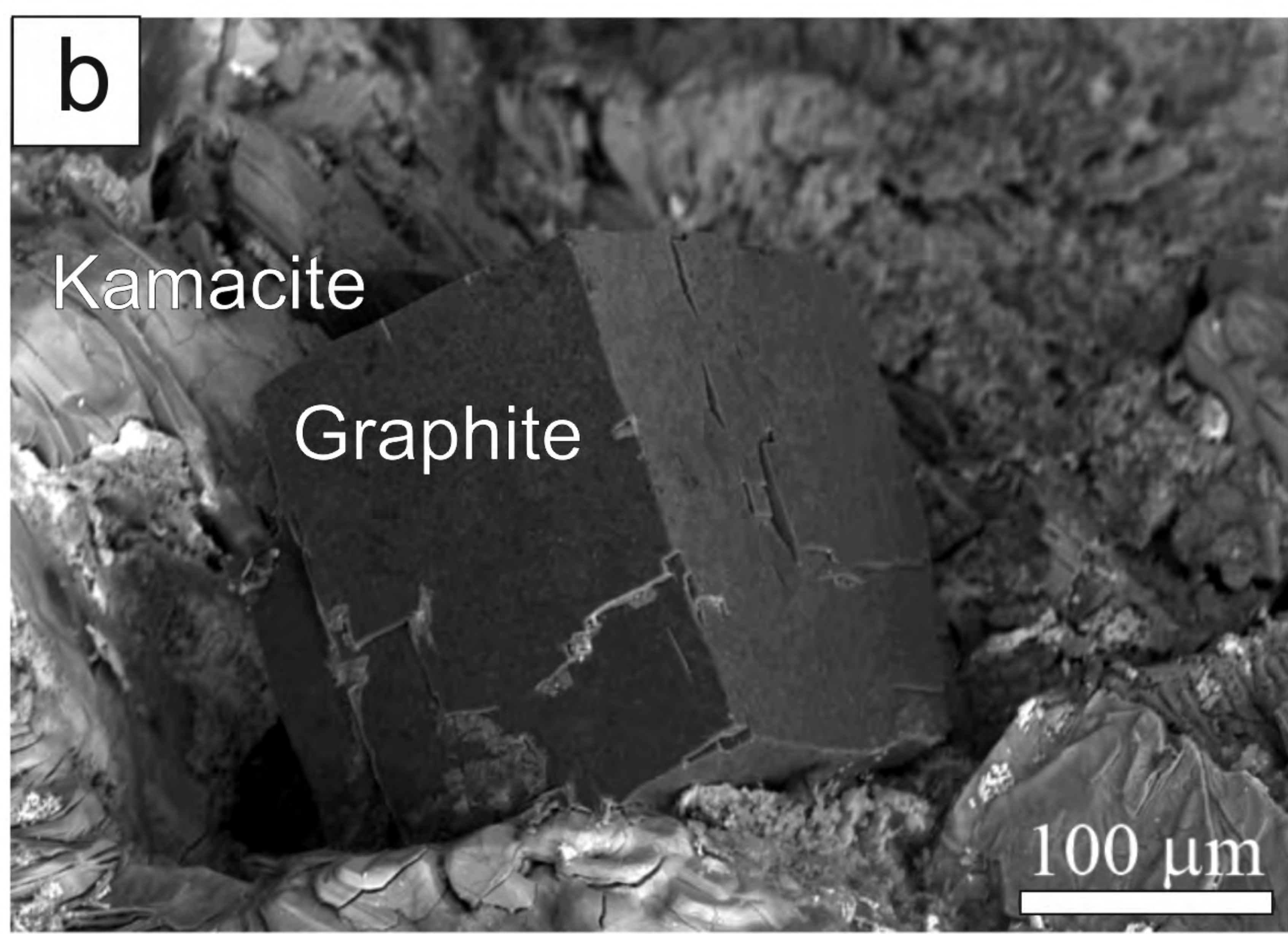
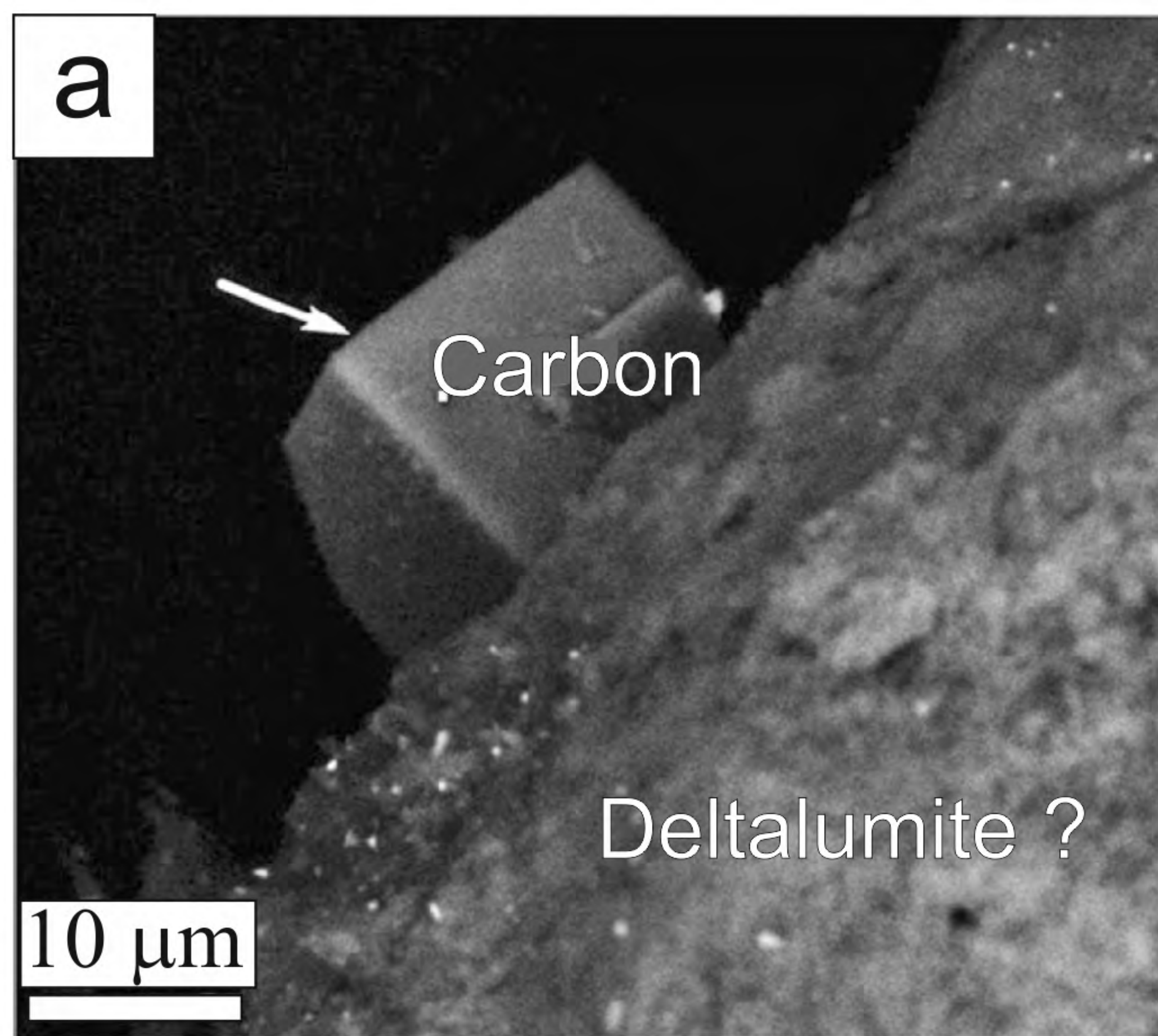
10 μm

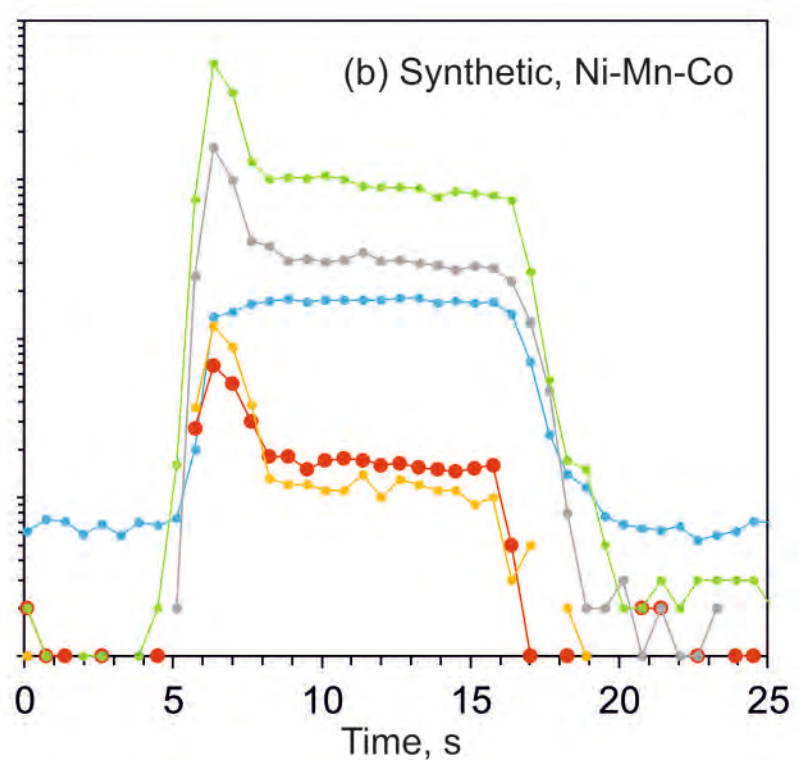
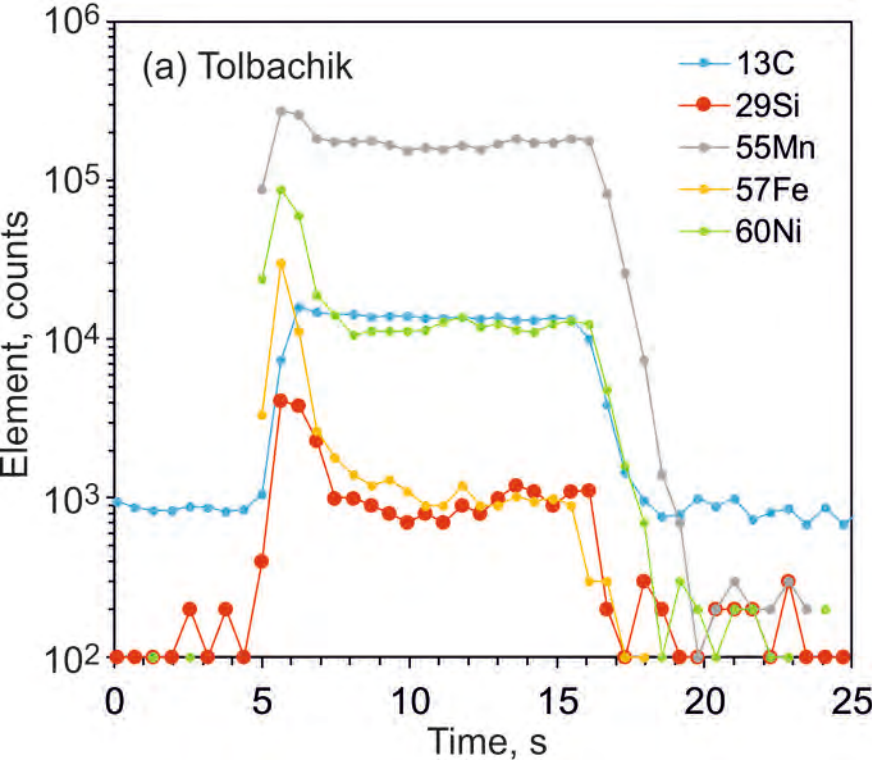
b

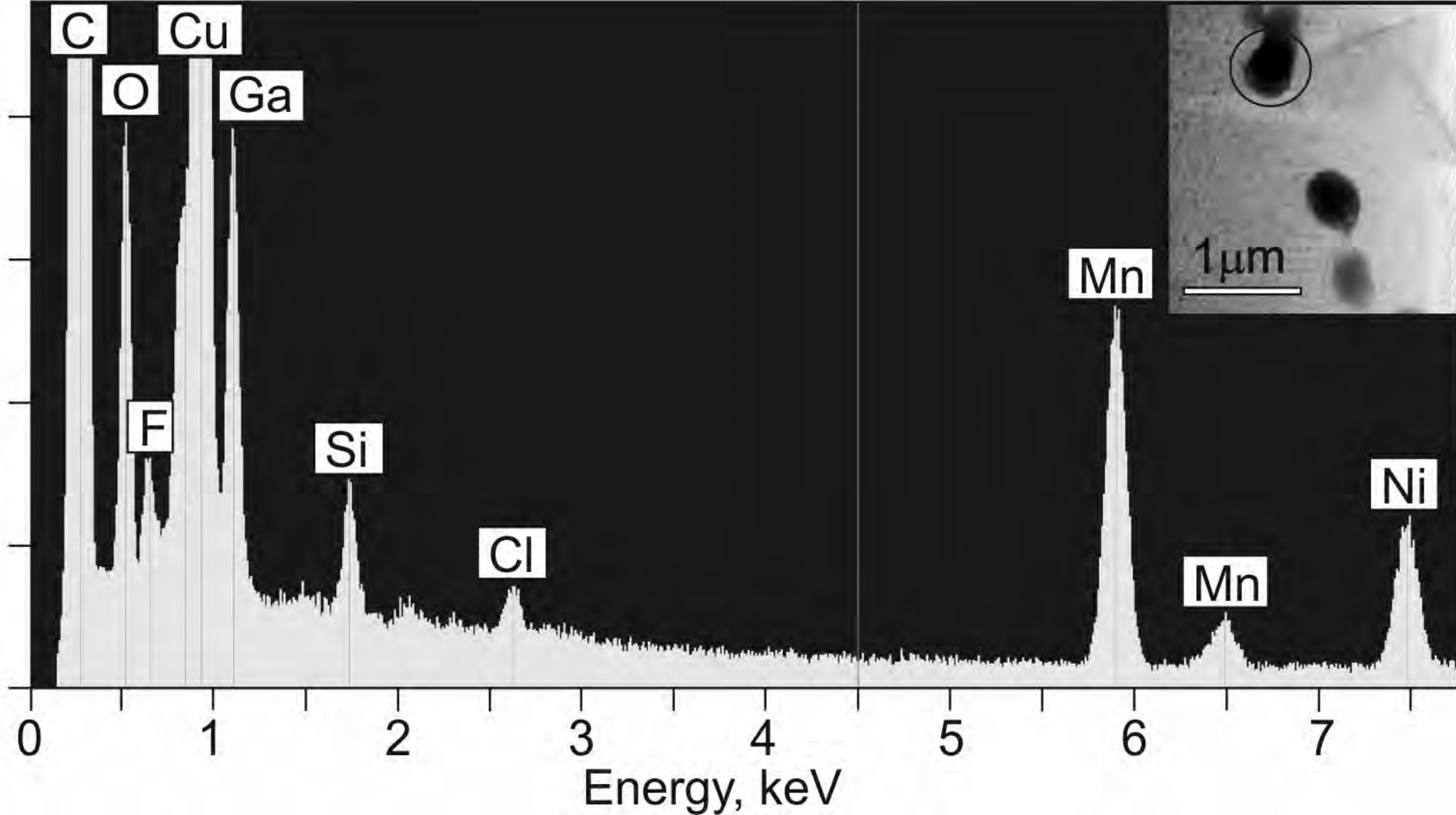
Kamacite

Graphite

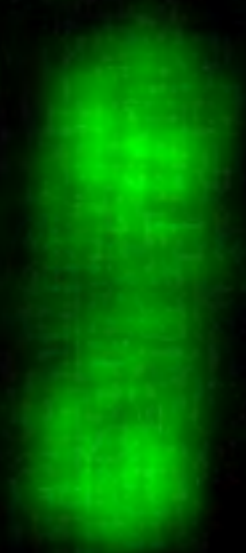
100 μm







Si



Cl



F



